PHYSICAL REVIEW D **87,** 016017 (2013)

Nucleon resonances in AdS/QCD

Thomas Gutsche,[1] Valery E. Lyubovitskij,[1,*] Ivan Schmidt,[2] and Alfredo Vega[3]

[1]*Institut für Theoretische Physik, Universität Tübingen, Kepler Center for Astro and Particle Physics, Auf der Morgenstelle 14, D-72076 Tübingen, Germany*

[2]*Departamento de Física y Centro Científico Tecnológico de Valparaíso (CCTVal), Universidad Técnica Federico Santa María, Casilla 110-V, Valparaíso, Chile*

[3]*Departamento de Física y Astronomía, Universidad de Valparaíso, Avenida Gran Bretaña 1111, Valparaíso, Chile*

(Received 28 December 2012; published 29 January 2013)

We describe the electroproduction of the $N(1440)$ Roper resonance in soft-wall anti–de Sitter/quantum chromodynamics. The Roper resonance is identified as the first radially excited state of the nucleon, where higher Fock states in addition to the three-quark ($3q$) component are included. The main conclusion is that the leading $3q$ component plays the dominant role in the description of electroproduction properties of this resonance: form factors, helicity amplitudes, and charge densities. The obtained results are in good agreement with the recent results of the CLAS Collaboration at JLab.

DOI: 10.1103/PhysRevD.87.016017 PACS numbers: 11.10.Kk, 13.40.Hq, 14.20.Dh, 14.20.Gk

I. INTRODUCTION

The study of electromagnetic properties of nucleon resonances, such as the Roper resonance, opens new opportunities for understanding the structure of hadrons. One of the more promising experiments of this type has been performed by the CLAS Collaboration at JLab [1,2], which will be continued at the upgraded JLab facilities with a 12-GeV energy beam [3]. This calls for a comprehensive theoretical analysis of this process. From the theoretical side, starting from 1980, different types of approaches/models [nonrelativistic and relativistic quark models, potential and hadronic molecular approaches, Dyson-Schwinger equation framework, light-front holographic quantum chromodynamics (QCD), etc.] have been proposed and developed for the description of electroexcitations of nucleon resonances [4–14] (for recent reviews see e.g., Refs. [10,12,14]). For example, in some recent theoretical developments [10,13] it is pointed out that a realistic description of the current data on Roper electroproduction needs to include additional degrees of freedom for this state, such as a nucleon-scalar σ meson molecular component. In Ref. [11] the Dirac form factor for the electromagnetic nucleon-Roper transition has been calculated in light-front holographic QCD.

In this paper we consider Roper electroproduction in a soft-wall anti–de Sitter/quantum chromodynamics (AdS/QCD) model [15–17], which not only includes the leading three-quark ($3q$) state but also higher Fock components. In Ref. [17] we proposed this AdS/QCD model as an approach to baryon structure, and successfully applied it to the study of nucleon electromagnetic form factors in the Euclidean region of transverse momentum squared up to 30 GeV^2. In Ref. [17] we found that the inclusion of higher Fock states is relevant for the quantitative reproduction of baryons properties—masses, and the electromagnetic form factors at small Q^2 including the electromagnetic radii. We truncated the tower of Fock states to the twist dimension $\tau = 5$, because the contribution of higher Fock states to the hadronic form factors scales as $(1/Q^2)^{\tau-1}$ at higher Q^2 and is therefore suppressed. Another reason for the truncation to $\tau = 5$ was to reduce the number of free parameters.

The paper is structured as follows. First, in Sec. II, we briefly discuss the basic notions of the approach. In Secs. III and IV we consider applications of our approach to the electroproduction of the Roper resonance. Finally, in Sec. V, we summarize our results.

II. APPROACH

A. Action for the spin $J = \frac{1}{2}$ fermion field in AdS space

Here we briefly review our approach. First, we specify the five-dimensional AdS metric:

$$\begin{aligned} ds^2 = g_{MN}dx^M dx^N &= \eta_{ab}e^{2A(z)}dx^a dx^b \\ &= e^{2A(z)}(\eta_{\mu\nu}dx^\mu dx^\nu - dz^2), \\ \eta_{\mu\nu} &= \mathrm{diag}(1,-1,-1,-1,-1), \end{aligned} \tag{1}$$

where M and $N = 0, 1, \ldots, 4$ are the space-time (base manifold) indices, $a = (\mu, z)$ and $b = (\nu, z)$ are the local Lorentz (tangent) indices, and g_{MN} and η_{ab} are curved and flat metric tensors, respectively, which are related by the vielbein $\epsilon^a_M(z) = e^{A(z)}\delta^a_M$ as $g_{MN} = \epsilon^a_M\epsilon^b_N\eta_{ab}$. Here z is the holographic coordinate, R is the AdS radius, and $g = |\det g_{MN}| = e^{10A(z)}$. In the following we restrict ourselves to a conformal-invariant metric with $A(z) = \log(R/z)$.

The relevant AdS/QCD action for the fermion field of twist τ is [17]

$$S_\tau = \int d^4x dz \sqrt{g} e^{-\varphi(z)} \sum_{i=+,-} \bar{\Psi}_{i,\tau}(x,z)\hat{\mathcal{D}}_i(z)\Psi_{i,\tau}(x,z), \tag{2}$$

*On leave of absence from Department of Physics, Tomsk State University, 634050 Tomsk, Russia.

where

$$\hat{\mathcal{D}}_{\pm}(z) = \frac{i}{2}\Gamma^M \overleftrightarrow{\partial}_M \mp (\mu + U_F(z)), \tag{3}$$

and $\Psi_{\pm,\tau}(x, z)$ is the pair of bulk fermion fields, which are the holographic analogues of the left- and right-chirality operators in the 4D theory. Here $A\overleftrightarrow{\partial}B \equiv A(\partial B) - (\partial A)B$, $\varphi(z) = \kappa^2 z^2$ is the dilaton field with κ being a free scale parameter. $\Gamma^M = \epsilon_a^M \Gamma^a$ and $\Gamma^a = (\gamma^\mu, -i\gamma^5)$ are the five-dimensional Dirac matrices (we use the chiral representation for the γ^μ and γ^5 matrices; see details in Refs. [15,17]). The quantity μ is the bulk fermion mass related to the scaling dimension τ as $m = \mu R = \tau - 3/2$. Note that the scaling dimension of the AdS fermion field is holographically identified with the scaling dimension of the baryon interpolating operator $\tau = N + L$; N is the number of partons in the baryon and $L = \max|L_z|$ is the maximal value of the z component of the quark orbital angular momentum in the light-front wave function [18,19]. $U_F(z) = \varphi(z)/R$ is the effective potential depending on the dilaton field. Its presence is necessary for the following reason. The form of the potential $U_F(z)$ is constrained in order to get solutions of the equations of motion (EOMs) for the fermionic Kaluza-Klein (KK) modes of left and right chirality, and to have the correct asymptotic behavior of the nucleon electromagnetic form factors at large Q^2 [15,17,20,21].

Notice that the fermion masses m and the effective potentials $U_F(z)$ corresponding to the fields Ψ_+ and Ψ_- have opposite signs according to the P-parity transformation (see details in Ref. [17]). The absolute sign of the fermion mass is related to the chirality of the boundary operator [22,23]. According to our conventions the QCD operators $\mathcal{O}_R$ and $\mathcal{O}_L$ have positive and negative chirality, and therefore the mass terms of the bulk fields Ψ_+ and Ψ_- have absolute signs "plus" and "minus," respectively. The fields Ψ_τ describe the AdS fermion field with different scaling dimension: $\tau = 3, 4, 5$, etc.

In Ref. [17] we demonstrated that our soft-wall holographic model reproduces the main features of the electromagnetic structure of the nucleon. In particular, we gained the following results: the analytical power scaling of the elastic nucleon form factors at large momentum transfers in accordance with quark-counting rules; reproduction of experimental data for magnetic moments and electromagnetic radii.

B. Mass spectrum

One advantage of the soft-wall AdS/QCD model is that most of the calculations can be done analytically. Here we show how in this approach the baryon spectrum and wave functions are generated following the procedure presented in Refs. [15,17,20,21]. First, we rescale the fermionic fields as

$$\Psi_{i,\tau}(x, z) = e^{\varphi(z)/2}\psi_{i,\tau}(x, z), \tag{4}$$

and remove the dilaton field from the overall exponential. In terms of the field $\psi_\tau(x, z)$ the modified action in the Lorentzian signature reads as

$$S_\tau = \int d^4x dz e^{4A(z)} \sum_{i=+,-} \bar{\psi}_{i,\tau}(x, z)\Big\{i\not{\partial} + \gamma^5\partial_z + 2A'(z)\gamma^5 - \delta_i \frac{e^{A(z)}}{R}(m + \varphi(z))\Big\}\psi_{i,\tau}(x, z), \tag{5}$$

where $\not{\partial} = \gamma^\mu\partial_\mu$, $\delta_\pm = \pm 1$. The fermion field $\psi_{i,\tau}(x, z)$ satisfies the following EOM [15,17,20,21]:

$$\left[i\not{\partial} + \gamma^5\partial_z + 2A'(z)\gamma^5 \mp \frac{e^{A(z)}}{R}(m + \varphi(z))\right]\psi_{\pm,\tau}(x, z) = 0. \tag{6}$$

Next we split the fermion field into left- and right-chirality components

$$\begin{aligned} \psi_{i,\tau}(x, z) &= \psi^L_{i,\tau}(x, z) + \psi^R_{i,\tau}(x, z), \\ \psi^{L/R}_{i,\tau}(x, z) &= \frac{1 \mp \gamma^5}{2}\psi_{i,\tau}(x, z), \\ \gamma^5\psi^{L/R}_{i,\tau}(x, z) &= \mp\psi^{L/R}_{i,\tau}(x, z), \end{aligned} \tag{7}$$

and perform a KK expansion for the $\psi^{L/R}_{i,\tau}(x, z)$ fields

$$\psi^{L/R}_{i,\tau}(x, z) = \frac{1}{\sqrt{2}}\sum_n \psi^{L/R}_n(x)F^{L/R}_{i,\tau,n}(z), \tag{8}$$

where $\psi^{L/R}_n(x)$ are the four-dimensional boundary fields (KK modes). These are Weyl spinors forming the Dirac bispinors $\psi_n(x) = \psi^L_n(x) + \psi^R_n(x)$, and $F^{L/R}_{i,\tau,n}(z)$ are the normalizable profile functions. Due to four-dimensional P- and C-parity invariance the bulk profiles are related as [17]

$$F^R_{\pm,\tau,n}(z) = \pm F^L_{\mp,\tau,n}(z). \tag{9}$$

Using this constraint, in the following we use the simplified notations:

$$\begin{aligned} F^R_{\tau,n}(z) &\equiv F^R_{+,\tau,n}(z) = F^L_{-,\tau,n}(z), \\ F^L_{\tau,n}(z) &\equiv F^L_{+,\tau,n}(z) = -F^R_{-,\tau,n}(z). \end{aligned} \tag{10}$$

Note that the profiles $F^{L/R}_{\tau,n}(z)$ are the holographic analogues of the nucleon wave functions with specific radial quantum number n and twist dimension τ (the latter corresponds to the specific partonic content of the nucleon Fock component), which satisfy the two coupled one-dimensional EOMs [17]:

$$\left[\partial_z \pm \frac{e^A}{R}(m + \varphi) + 2A'\right]F^{L/R}_{n,\tau}(z) = \pm M_{n\tau}F^{R/L}_{n,\tau}(z). \tag{11}$$

Therefore, the main aim is to find solutions for the bulk profiles of the AdS field in the z direction and then

calculate the physical properties of hadrons. After straightforward algebra one can obtain the decoupled EOMs:

$$\left[-\partial_z^2 - 4A'\partial_z + \frac{e^{2A}}{R^2}(m+\varphi)^2 \mp \frac{e^A}{R}(A'(m+\varphi)+\varphi') - 4A'^2 - 2A''\right]F_{\tau,n}^{L/R}(z) = M_{n\tau}^2 F_{\tau,n}^{L/R}(z). \quad (12)$$

Performing the substitution

$$F_{\tau,n}^{L/R}(z) = e^{-2A(z)} f_{\tau,n}^{L/R}(z), \quad (13)$$

we derive the Schrödinger-type EOM for $f_{\tau,n}^{L/R}(z)$

$$\left[-\partial_z^2 + \frac{e^{2A}}{R^2}(m+\varphi)^2 \mp \frac{e^A}{R}(A'(m+\varphi)+\varphi')\right]f_{\tau,n}^{L/R}(z) = M_{n\tau}^2 f_{\tau,n}^{L/R}(z). \quad (14)$$

For $A(z) = \log(R/z)$, $\varphi(z) = \kappa^2 z^2$ we get

$$\left[-\partial_z^2 + \kappa^4 z^2 + 2\kappa^2\left(m \mp \frac{1}{2}\right) + \frac{m(m\pm 1)}{z^2}\right]f_{\tau,n}^{L/R}(z) = M_{n\tau}^2 f_{\tau,n}^{L/R}(z), \quad (15)$$

where

$$f_{\tau,n}^{L}(z) = \sqrt{\frac{2\Gamma(n+1)}{\Gamma(n+\tau)}}\kappa^\tau z^{\tau-1/2} e^{-\kappa^2 z^2/2} L_n^{\tau-1}(\kappa^2 z^2), \quad (16)$$

$$f_{\tau,n}^{R}(z) = \sqrt{\frac{2\Gamma(n+1)}{\Gamma(n+\tau-1)}}\kappa^{\tau-1} z^{\tau-3/2} e^{-\kappa^2 z^2/2} L_n^{\tau-2}(\kappa^2 z^2), \quad (17)$$

and

$$M_{n\tau}^2 = 4\kappa^2(n+\tau-1), \quad (18)$$

with

$$\int_0^\infty dz f_{\tau,n_1}^{L/R}(z) f_{\tau,n_2}^{L/R}(z) = \delta_{n_1 n_2}. \quad (19)$$

Here

$$L_n^\tau(x) = \frac{x^{-\tau}e^x}{n!}\frac{d^n}{dx^n}(e^{-x}x^{\tau+n}), \quad (20)$$

are the generalized Laguerre polynomials. In the above formulas we substituted $m = \tau - 3/2$.

One can see that the functions $F_{\tau,n}^{L/R}(z) = e^{-2A(z)} f_{\tau,n}^{L/R}(z)$ have the correct scaling behavior for small z

$$F_{\tau,n}^{L}(z) \sim z^{\tau+3/2}, \qquad F_{\tau,n}^{R}(z) \sim z^{\tau+1/2}, \quad (21)$$

when identified with the corresponding nucleon wave functions with twist τ and vanish at large z (confinement). In Ref. [17] it was explicitly demonstrated that the nucleon electromagnetic form factors have the correct scaling dependence at large Q^2.

Now we define the 5D fields $\psi_{\pm,\tau}^N(x,z)$ and $\psi_{\pm,\tau}^{\mathcal{R}}(x,z)$, which are holographic analogues of the nucleon and Roper resonance, respectively:

$$\psi_{\pm,\tau}^N(x,z) = \frac{1}{\sqrt{2}}[\psi_0^L(x)F_{\tau,0}^{L/R}(z) \pm \psi_0^R(x)F_{\tau,0}^{R/L}(z)],$$
$$\psi_{\pm,\tau}^{\mathcal{R}}(x,z) = \frac{1}{\sqrt{2}}[\psi_1^L(x)F_{\tau,1}^{L/R}(z) \pm \psi_1^R(x)F_{\tau,1}^{R/L}(z)]. \quad (22)$$

Here we identify the nucleon as the ground state with $n = 0$ and the Roper resonance as the first radially excited state with $n = 1$. We should stress again that 5D AdS fields corresponding to the nucleon and Roper are products of 4D spinor fields with spin $1/2$ and profiles depending on the holographic (scale) variable. The free actions of the nucleon and Roper resonance with fixed twist dimension τ are constructed in terms of $\psi_{\pm,\tau}^N(x,z)$ and $\psi_{\pm,\tau}^{\mathcal{R}}(x,z)$ as

$$S_\tau^B = \int d^4x dz e^{4A(z)} \sum_{i=+,-} \bar{\psi}_{i,\tau}^B(x,z)\Big\{i\not{\partial} + \gamma^5\partial_z + 2A'(z)\gamma^5 - \delta_i\frac{e^{A(z)}}{R}(m+\varphi(z))\Big\}\psi_{i,\tau}^B(x,z), \quad (23)$$

where $B = N, \mathcal{R}$. In order to take into account higher Fock states in both the nucleon and Roper we sum the 5D action S_τ^B over τ with adjustable coefficients c_τ^B:

$$S^B = \sum_\tau c_\tau^B S_\tau^B. \quad (24)$$

In Ref. [17] we showed that the c_τ^B are constrained by the condition $\sum_\tau c_\tau^B = 1$ in order to get the correct normalization of the kinetic term $\bar{\psi}_n(x)i\not{\partial}\psi_n(x)$ of the four-dimensional spinor field. Also this condition is consistent with electromagnetic gauge invariance.

The nucleon and Roper masses are identified with the expressions [17]

$$M_N = 2\kappa\sum_\tau c_\tau^N\sqrt{\tau-1}, \qquad M_{\mathcal{R}} = 2\kappa\sum_\tau c_\tau^{\mathcal{R}}\sqrt{\tau}. \quad (25)$$

Integration over the holographic coordinate z, with the use of the normalization condition (19) for the profile functions $f_{\tau,n}^{L/R}(z)$, gives four-dimensional actions for the fermion field $\psi_n(x) = \psi_n^L(x) + \psi_n^R(x)$ with $n = 0$ (for nucleon) and $n = 1$ (for Roper):

$$S_{4D}^B = \int d^4x\,\bar{\psi}_0(x)[i\not{\partial} - M_N]\psi_0(x) + \int d^4x\,\bar{\psi}_1(x)[i\not{\partial} - M_{\mathcal{R}}]\psi_1(x). \quad (26)$$

This last equation is a manifestation of the gauge-gravity duality. It explicitly demonstrates that effective actions for conventional hadrons in four dimensions can be generated from actions for bulk fields propagating in five-dimensional AdS space. The effect of the extra dimension is encoded in the baryon mass M_B.

In the following we restrict ourselves to the contribution of Fock states in both the nucleon and the Roper resonance with twist $\tau = 3$, 4 and 5. The nucleon mass was already calculated in Ref. [17]. Taking the following choice of parameters κ, c_3^N, and c_4^N:

$$\kappa = 383 \text{ MeV}, \qquad c_3^N = 1.25, \qquad c_4^N = 0.16, \tag{27}$$

we reproduce the data for the nucleon (proton) mass $M_N^{\text{exp}} = 938.27$ MeV. Notice that the parameter c_5^N depends on c_3^N and c_4^N as

$$c_5^N = 1 - c_3^N - c_4^N = -0.41. \tag{28}$$

Taking the same value of the universal scale parameter $\kappa = 383$ MeV we reproduce the world average for the Roper mass $M_{\mathcal{R}}^{\text{exp}} = 1440$ MeV with

$$\begin{aligned} c_3^{\mathcal{R}} &= 0.78, \qquad c_4^{\mathcal{R}} = -0.16, \\ c_5^{\mathcal{R}} &= 1 - c_3^{\mathcal{R}} - c_4^{\mathcal{R}} = 0.38. \end{aligned} \tag{29}$$

One can see that, as in the nucleon case, the $3q$ Fock component gives the main contribution to the Roper mass.

We would like to stress again that the quantities c_τ^B ($B = N, \mathcal{R}$) are free parameters constrained by the condition $\sum_\tau c_\tau^B = 1$. Inclusion of the states for $\tau = 6$ does not change qualitatively the description of data. On the other hand, from the analysis of data on nucleon form factors, nucleon, and Roper mass, we found that the contribution of twist-4 Fock states (containing three quarks and one gluon) is always suppressed in comparison with leading $3q$ component and twist-5 Fock states containing a sizeable $3q + q\bar{q}$ component.

Next we will study the role of different Fock components in the electroproduction properties of the Roper resonance.

III. ELECTROPRODUCTION OF THE ROPER RESONANCE $N + \gamma^* \to \mathcal{R}$

A. Kinematics

The electromagnetic transition between the nucleon and the Roper resonance, due to Lorentz and gauge invariance, is defined by the following matrix element:

$$\begin{aligned} M^\mu(p_1, \lambda_1; p_2, \lambda_2) &= \bar{u}_{\mathcal{R}}(p_1, \lambda_1)\Big[\gamma_\perp^\mu F_1(q^2) \\ &\quad + i\sigma^{\mu\nu}\frac{q_\nu}{M_{\mathcal{R}}} F_2(q^2)\Big] u_N(p_2, \lambda_2), \\ \gamma_\perp^\mu &= \gamma^\mu - q^\mu \frac{q}{q^2}, \end{aligned} \tag{30}$$

which obeys current conservation

$$q_\mu M^\mu = 0, \tag{31}$$

where (p_1, λ_1), (p_2, λ_2), $(q = p_1 - p_2, \lambda = \lambda_1 + \lambda_2)$ are the (momenta, helicity) of the Roper resonance, the nucleon, and the photon, respectively. We shall work in the rest frame of the daughter baryon (Roper) with the parent baryon (nucleon) moving in the negative z direction (z axis is directed along the photon 3-momentum):

$$\begin{aligned} p_1^\mu &= (M_{\mathcal{R}}, \vec{\mathbf{0}}), \qquad p_2^\mu = (E, 0, 0, -|\mathbf{p}|), \\ q^\mu &= (q_0, 0, 0, |\mathbf{p}|), \end{aligned} \tag{32}$$

where

$$\begin{aligned} E &= \frac{Q_+}{2M_{\mathcal{R}}} - M_N, \qquad |\mathbf{p}| = \frac{\sqrt{Q_+ Q_-}}{2M_{\mathcal{R}}}, \\ Q_\pm &= M_\pm^2 + Q^2, \qquad M_\pm = M_{\mathcal{R}} \pm M_N, \\ Q^2 &= -q^2. \end{aligned} \tag{33}$$

Alternative sets of transition form factors can be found in Refs. [5,6,9].

Now we introduce the helicity amplitudes $H_{\lambda_2\lambda}$, which in turn can be related to the invariant form factors F_i (see details in Refs. [24–26]). The pertinent relation is

$$H_{\lambda_2\lambda} = M_\mu(p_1, \lambda_1; p_2, \lambda_2)\epsilon^{*\mu}(q, \lambda), \tag{34}$$

where the polarization vectors of the outgoing photon $\epsilon^{*\mu}(q, \lambda)$ are written as

$$\begin{aligned} \epsilon^{*\mu}(q, \pm 1) &= \frac{1}{\sqrt{2}}(0, \mp 1, i, 0), \\ \epsilon^{*\mu}(q, 0) &= \frac{1}{\sqrt{Q^2}}(|\mathbf{p}|, 0, 0, q_0). \end{aligned} \tag{35}$$

The $J = \frac{1}{2}$ baryon spinors are given by

$$\begin{aligned} \bar{u}_{\mathcal{R}}\left(p_1, \pm\frac{1}{2}\right) &= \sqrt{2M_{\mathcal{R}}}(\chi_\pm^\dagger, 0), \\ u_N\left(p_2, \mp\frac{1}{2}\right) &= \sqrt{E + M_N}\begin{pmatrix} \chi_\pm \\ \frac{\mp|\mathbf{p}|}{E+M_N}\chi_\pm \end{pmatrix}. \end{aligned} \tag{36}$$

Here $\chi_+ = \binom{1}{0}$ and $\chi_- = \binom{0}{1}$ are two-component Pauli spinors.

After straightforward calculations [24–26] we find

$$H_{\pm\frac{1}{2}0} = \sqrt{\frac{Q_-}{Q^2}}\left(F_1 M_+ - F_2 \frac{Q^2}{M_{\mathcal{R}}}\right), \tag{37}$$

$$H_{\pm\frac{1}{2}\pm 1} = -\sqrt{2Q_-}\left(F_1 + F_2 \frac{M_+}{M_{\mathcal{R}}}\right). \tag{38}$$

The alternative set of the helicity amplitudes $(A_{1/2}, S_{1/2})$ is related to the set $(H_{\frac{1}{2}0}, H_{\frac{1}{2}1})$ as [5–9]

$$A_{1/2} = -bH_{\frac{1}{2}1}, \qquad S_{1/2} = b\frac{|\mathbf{p}|}{\sqrt{Q^2}}H_{\frac{1}{2}0}, \tag{39}$$

where

$$b = \sqrt{\frac{\pi\alpha}{M_+ M_- M_N}}, \tag{40}$$

and $\alpha = 1/137.036$ is the fine-structure constant.

B. Form factors of the $N + \gamma \to \mathcal{R}$ transition

In our approach the matrix element describing the $N + \gamma \to \mathcal{R}$ transition is generated by the following 5d action:

$$S_{\rm int} = \int d^4x dz \sqrt{g} e^{-\varphi(z)} \mathcal{L}_{\rm int}(x, z). \tag{41}$$

$\mathcal{L}_{\rm int}(x, z)$ is the interaction Lagrangian of two fermion fields (holographically corresponding to the nucleon and Roper resonance) and vector field (holographically corresponding to the electromagnetic field):

$$\mathcal{L}_{\rm int}(x, z) = \sum_{i=+,-;\tau} c_\tau^{\mathcal{R}N} \bar{\psi}^{\mathcal{R}}_{i,\tau}(x, z) \hat{\mathcal{V}}_i(x, z) \psi^N_{i,\tau}(x, z) + \text{H.c.},$$

$$\hat{\mathcal{V}}_\pm(x, z) = \tau_3 \Gamma^M V_M(x, z) \pm \frac{i}{4} \eta_V [\Gamma^M, \Gamma^N] V_{MN}(x, z) \pm g_V \tau_3 \Gamma^M i \Gamma^z V_M(x, z), \tag{42}$$

where $c_\tau^{\mathcal{R}N}$ is the set of parameters mixing the contribution of AdS fermion fields with different twist dimension. Here $\eta_V = \text{diag}(\eta_p, \eta_n)$ and τ_3 is the Pauli isospin matrix, η_p, η_n, g_V are the coupling constants, $V_M(x, z)$ is the AdS vector field, and $V_{MN} = \partial_M V_N - \partial_N V_M$ is its stress tensor.

The expressions for the F_1 and F_2 form factors are given by

$$F_1^p(Q^2) = C_1(Q^2) + g_V C_2(Q^2) + \eta_p C_3(Q^2), \tag{43}$$

$$F_2^p(Q^2) = \eta_p C_4(Q^2), \tag{44}$$

for the case of $p + \gamma \to \mathcal{R}_p$ transition, and

$$F_1^n(Q^2) = -C_1(Q^2) - g_V C_2(Q^2) + \eta_n C_3(Q^2), \tag{45}$$

$$F_2^n(Q^2) = \eta_n C_4(Q^2), \tag{46}$$

for the case of $n + \gamma \to \mathcal{R}_n$ transition. Here, $\mathcal{R}_p$ and $\mathcal{R}_n$ are the members of the Roper isospin doublet, and $C_i(Q^2)$ are the structure integrals (see explicit expressions in the Appendix):

$$C_1(Q^2) = \frac{1}{2} \int_0^\infty dz V(Q, z) \sum_\tau c_\tau^{\mathcal{R}N} (f^L_{\tau,0}(z) f^L_{\tau,1}(z) + f^R_{\tau,0}(z) f^R_{\tau,1}(z)),$$

$$C_2(Q^2) = \frac{1}{2} \int_0^\infty dz V(Q, z) \sum_\tau c_\tau^{\mathcal{R}N} (f^R_{\tau,0}(z) f^R_{\tau,1}(z) - f^L_{\tau,0}(z) f^L_{\tau,1}(z)),$$

$$C_3(Q^2) = \frac{1}{2} \int_0^\infty dz z \partial_z V(Q, z) \sum_\tau c_\tau^{\mathcal{R}N} (f^L_{\tau,0}(z) f^L_{\tau,1}(z) - f^R_{\tau,0}(z) f^R_{\tau,1}(z)),$$

$$C_4(Q^2) = \frac{M_+}{2} \int_0^\infty dz z V(Q, z) \sum_\tau c_\tau^{\mathcal{R}N} (f^L_{\tau,0}(z) f^R_{\tau,1}(z) + f^L_{\tau,1}(z) f^R_{\tau,0}(z)). \tag{47}$$

The functions $f^{R/L}_{\tau,n=0,1}(z)$ are the bulk profiles of fermions with specific $n = 0$ or 1. $V(Q, z)$ is the bulk-to-boundary propagator of the transverse massless vector bulk field (the holographic analogue of the electromagnetic field) defined as

$$V_\mu(x, z) = \int \frac{d^4q}{(2\pi)^4} e^{-iqx} V_\mu(q) V(q, z), \tag{48}$$

which obeys the following EOM:

$$\partial_z \left(\frac{e^{-\varphi(z)}}{z} \partial_z V(q, z) \right) + q^2 \frac{e^{-\varphi(z)}}{z} V(q, z) = 0. \tag{49}$$

In the soft-wall model the solution for $V(Q, z)$ is given in analytical form in terms of the gamma $\Gamma(n)$ and Tricomi $U(a, b, z)$ functions:

$$V(Q, z) = \Gamma\left(1 + \frac{Q^2}{4\kappa^2}\right) U\left(\frac{Q^2}{4\kappa^2}, 0, \kappa^2 z^2\right). \tag{50}$$

The bulk-to-boundary propagator $V(Q, z)$ obeys the normalization condition $V(0, z) = 1$, consistent with gauge invariance, and fulfills the following ultraviolet (UV) and infrared (IR) boundary conditions:

$$V(Q, 0) = 1, \qquad V(Q, \infty) = 0. \tag{51}$$

The UV boundary condition corresponds to the local (structureless) coupling of the electromagnetic field to matter fields, while the IR boundary condition implies that the vector field vanishes at $z = \infty$.

In order to obtain analytical expressions for the functions $C_i(Q^2)$, it is convenient to use the integral representation for $V(Q, z)$ introduced in Ref. [27]

$$V(Q, z) = \kappa^2 z^2 \int_0^1 \frac{dx}{(1 - x)^2} x^{\frac{Q^2}{4\kappa^2}} e^{-\frac{\kappa^2 z^2 x}{1-x}}, \tag{52}$$

where the variable x is equivalent to the light-cone momentum fraction [28].

There are a few very important properties of the $C_i(Q^2)$ functions. Namely, at $Q^2 = 0$ they are normalized as

$$C_1(0) = C_2(0) = C_3(0) = 0, \qquad C_4(0) = -\frac{M_+}{2} \sum_\tau c_\tau^{\mathcal{R}N}. \tag{53}$$

The normalizations of C_i ($i = 1, 2, 3$) are consistent with gauge invariance.

The analytical power scaling of the $C_i(Q^2)$ functions and therefore of the form factors $F_i^N(Q^2)$, defining the electromagnetic transition between nucleon and Roper resonance, is in accordance with quark-counting rules for large momentum transfers. In particular, the leading $3q$ contribution in $C_i(Q^2)$ and $F_i^N(Q^2)$ scales for $Q^2 \to \infty$ as

$$C_1(Q^2) \sim C_2(Q^2) \sim C_3(Q^2) \sim \frac{1}{Q^4}, \qquad C_4(Q^2) \sim \frac{1}{Q^6}, \tag{54}$$

and

$$F_1^N(Q^2) \sim \frac{1}{Q^4}, \qquad F_2^N(Q^2) \sim \frac{1}{Q^6}, \tag{55}$$

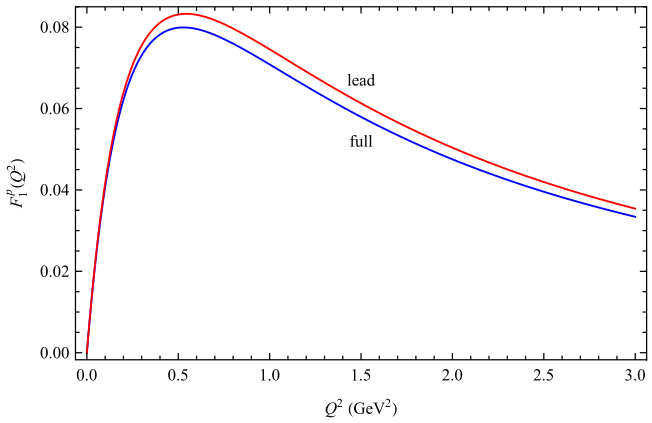

FIG. 1 (color online). $F_1^p(Q^2)$ form factor.

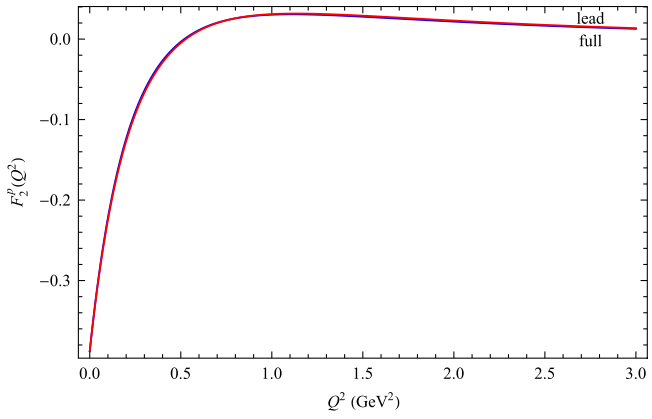

FIG. 2 (color online). $F_2^p(Q^2)$ form factor.

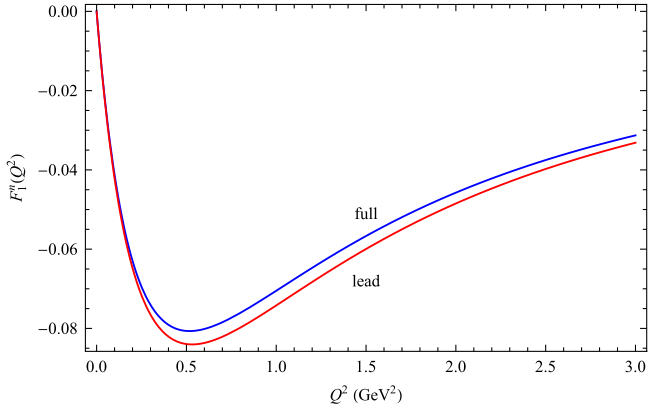

FIG. 3 (color online). $F_1^n(Q^2)$ form factor.

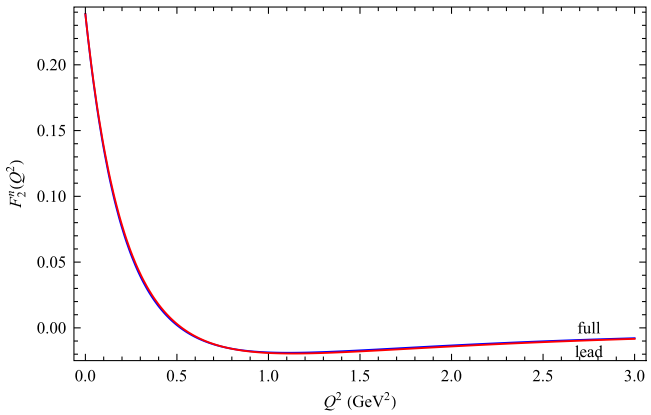

FIG. 4 (color online). $F_2^n(Q^2)$ form factor.

for the case of $p + \gamma \to \mathcal{R}_p$ transition, and similarly for

$$F_1^n(Q^2) = -C_1(Q^2) - g_V C_2(Q^2) + \eta_n C_3(Q^2), \tag{56}$$

$$F_2^n(Q^2) = \eta_n C_4(Q^2). \tag{57}$$

Following Ref. [9] we define the transition charge density for the unpolarized $N \to R$ transition:

$$\rho_0(\vec{b}_\perp) = \int \frac{d^2\vec{q}_\perp}{(2\pi)^2} e^{-i\vec{q}_\perp \vec{b}_\perp} \frac{1}{2P^+} \times \left\langle P^+, \frac{\vec{q}_\perp}{2}, \lambda | J^+(0) | P^+, -\frac{\vec{q}_\perp}{2}, \lambda \right\rangle, \tag{58}$$

and for the transversely polarized nucleon and Roper resonance, both along the direction of $\vec{S}_\perp = \cos\phi_S \hat{e}_x + \sin\phi_S \hat{e}_y$:

$$\rho_T(\vec{b}_\perp) = \int \frac{d^2\vec{q}_\perp}{(2\pi)^2} e^{-i\vec{q}_\perp \vec{b}_\perp} \frac{1}{2P^+} \times \left\langle P^+, \frac{\vec{q}_\perp}{2}, s_\perp | J^+(0) | P^+, -\frac{\vec{q}_\perp}{2}, s_\perp \right\rangle, \tag{59}$$

where $\vec{b}_\perp$ is the position in the (xy) plane from transverse c.m. of the baryons and $s_\perp$ is the nucleon spin projection along the direction of $\vec{S}_\perp$.

IV. RESULTS

In this section we present the numerical analysis of the physical observables of the electromagnetic nucleon-Roper transition: form factors, helicity amplitudes, and

TABLE I. Helicity amplitudes $A_{1/2}^N(0)$ and $S_{1/2}^N(0)$, $N = p, n$: full results and leading 3q contributions (in brackets).

Quantity	Our results	Data [29]
$A_{1/2}^p(0)$ (GeV$^{-1/2}$)	-0.065 (-0.065)	-0.065 ± 0.004
$A_{1/2}^n(0)$ (GeV$^{-1/2}$)	0.040 (0.040)	0.040 ± 0.010
$S_{1/2}^p(0)$ (GeV$^{-1/2}$)	0.047 (0.048)	
$S_{1/2}^n(0)$ (GeV$^{-1/2}$)	-0.044 (-0.045)	

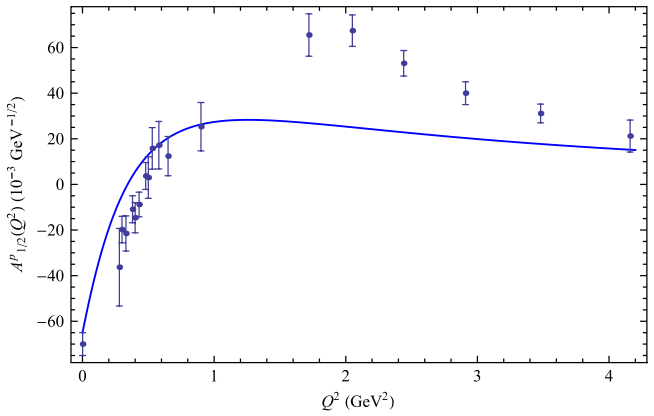

FIG. 5 (color online). Helicity amplitude $A^p_{1/2}(Q^2)$ up to $Q^2 = 4$ GeV^2.

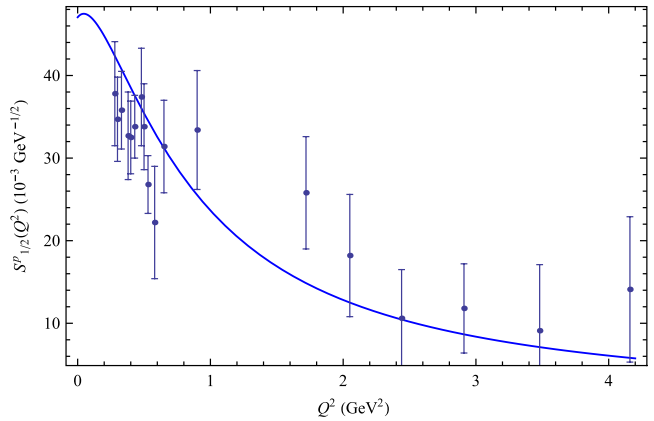

FIG. 6 (color online). Helicity amplitude $S^p_{1/2}(Q^2)$ up to $Q^2 = 4$ GeV^2.

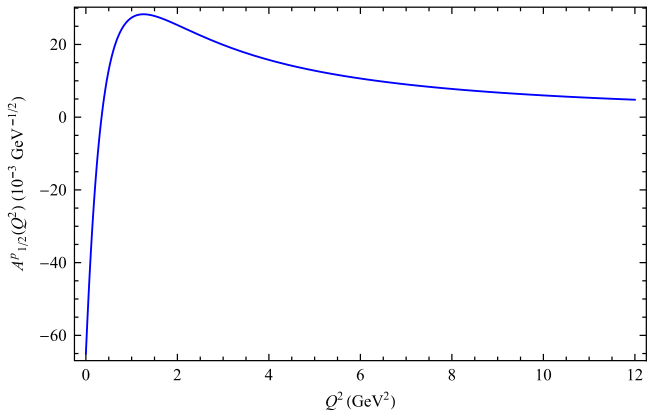

FIG. 7 (color online). Helicity amplitude $A^p_{1/2}(Q^2)$ up to $Q^2 = 12$ GeV^2.

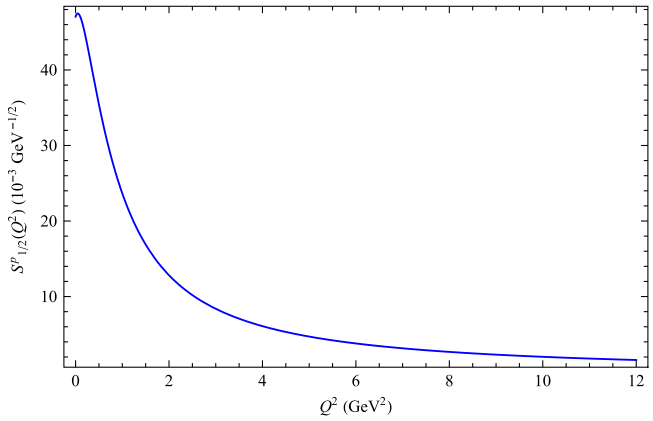

FIG. 8 (color online). Helicity amplitude $S^p_{1/2}(Q^2)$ up to $Q^2 = 12$ GeV^2.

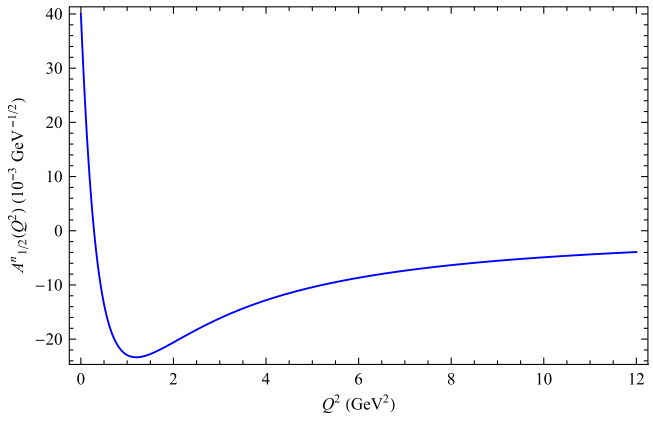

FIG. 9 (color online). Helicity amplitude $A^n_{1/2}(Q^2)$ up to $Q^2 = 12$ GeV^2.

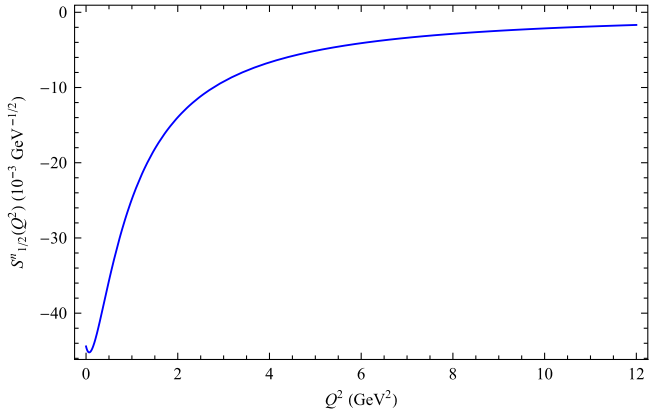

FIG. 10 (color online). Helicity amplitude $S^n_{1/2}(Q^2)$ up to $Q^2 = 12$ GeV^2.

transition charge radii. As in the case of the nucleon electromagnetic form factors, for the electroproduction of the Roper resonance the main contribution is given by the leading $3q$ component. The higher Fock components compensate each other. We illustrate this feature in Figs. 1–4. In particular, the plots of the leading ($3q$ Fock component) and full results (including $3q$, 4, and 5 partonic contributions) practically coincide. In Table I we present full results and leading $3q$ contributions (in brackets) for the helicity amplitudes $A^N_{1/2}(0)$ and $S^N_{1/2}(0)$, $N = p, n$.

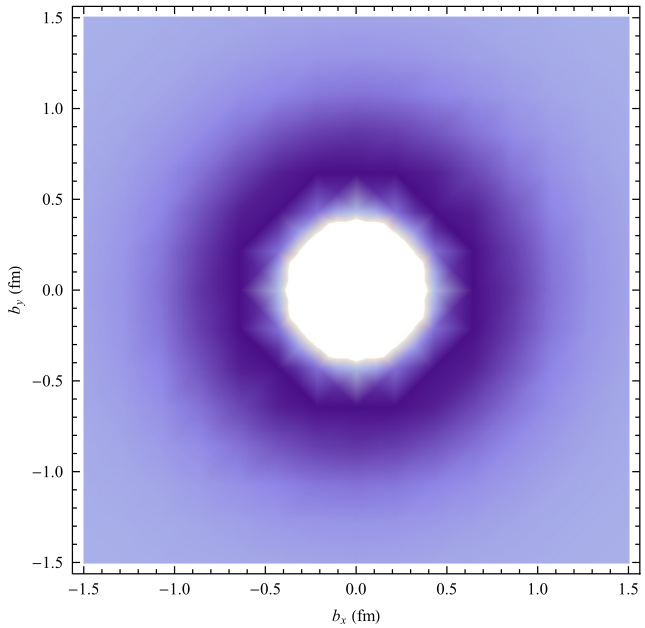

FIG. 11 (color online). Charge density $\rho_0^p(b_x, b_y)$.

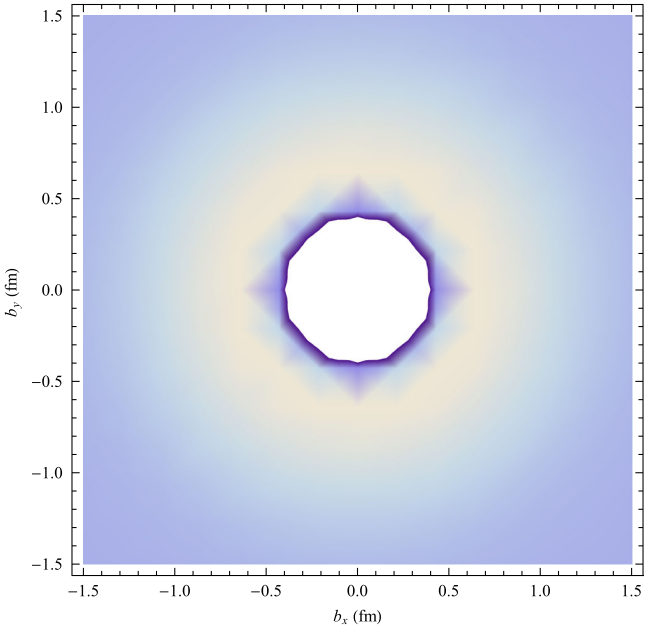

FIG. 13 (color online). Charge density $\rho_0^n(b_x, b_y)$.

Finally, the free parameters are fixed as

$$g_V = 1, \qquad \eta_p = 0.453, \qquad \eta_n = -0.279,$$
$$c_3^{\mathcal{R}N} = 0.72, \qquad c_4^{\mathcal{R}N} = -c_5^{\mathcal{R}N} = -0.18. \tag{60}$$

From Figs. 5 and 6 it should be evident that our results for the helicity amplitudes in the proton case have qualitative agreement with the present data of the CLAS Collaboration [1]. Within the current approach it is difficult to reproduce the maximum of data for $A_{1/2}^p$ at about 2 GeV^2. Higher-twist contributions cannot improve this situation as discussed before. We recently proposed an extension of our soft-wall model including a longitudinal wave function in the case of mesons. In the future we plan to do a similar extension in the baryon sector, which can help to improve the fit in the intermediate Q^2 region. Further data for the helicity amplitudes in the region from 1.6 to 4 GeV^2 could be accumulated at the upgraded facilities of JLab and certainly help to clarify the theoretical understanding. In Figs. 7–10 we show our predictions for the proton- and neutron-case helicities up to 12 GeV^2.

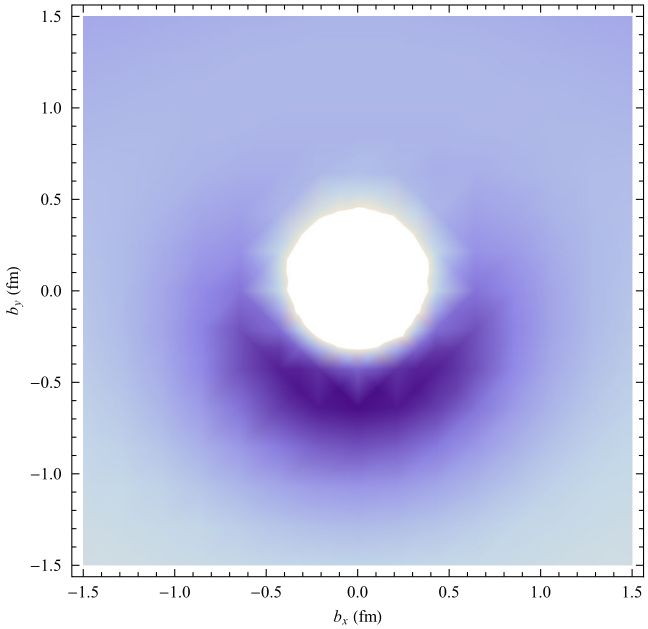

FIG. 12 (color online). Charge density $\rho_T^p(b_x, b_y)$.

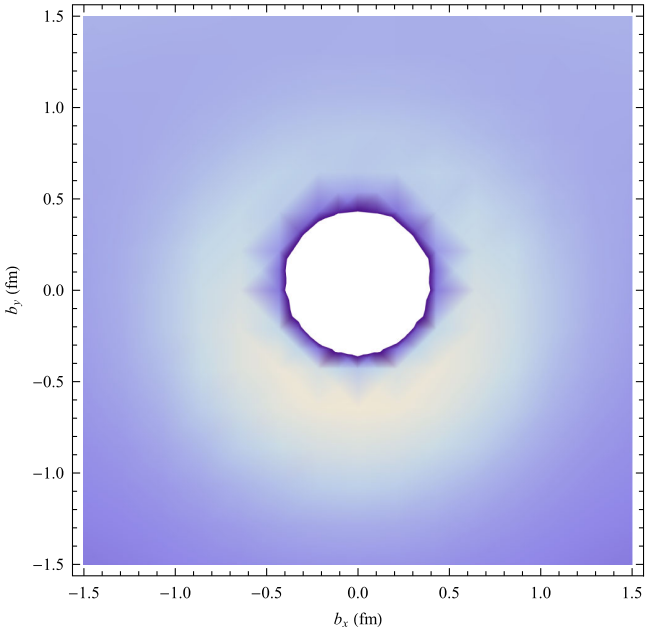

FIG. 14 (color online). Charge density $\rho_T^n(b_x, b_y)$.

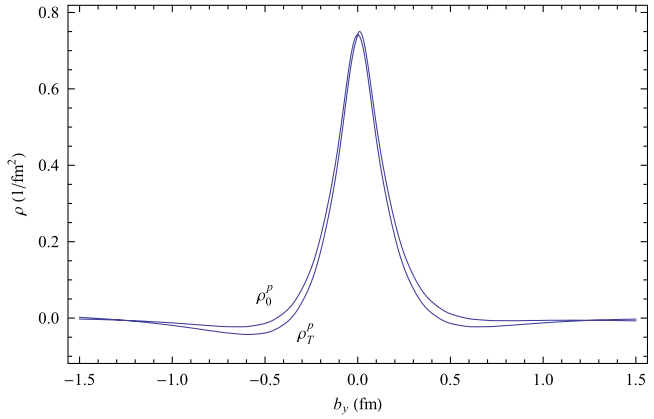

FIG. 15 (color online). Charge densities $\rho_0^p(b_y)$ and $\rho_T^p(b_y)$.

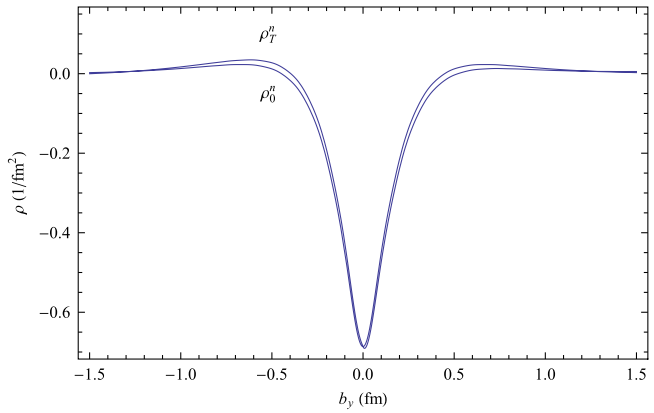

FIG. 16 (color online). Charge densities $\rho_0^n(b_y)$ and $\rho_T^n(b_y)$.

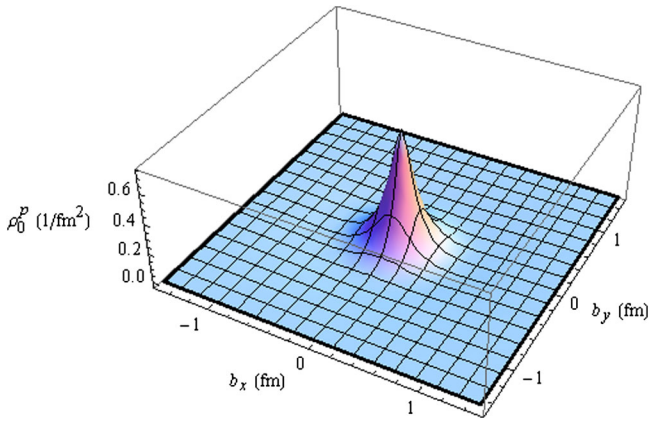

FIG. 17 (color online). 3D image of $\rho_0^p(b_x, b_y)$.

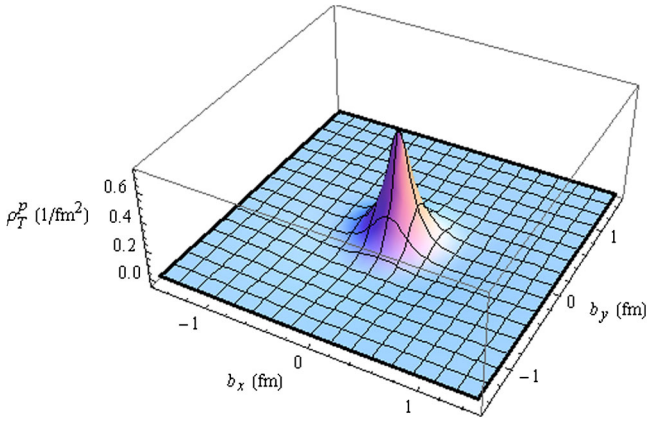

FIG. 18 (color online). 3D image of $\rho_T^p(b_x, b_y)$.

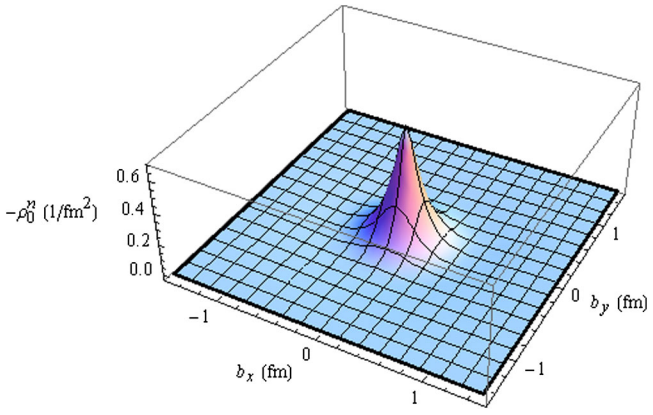

FIG. 19 (color online). 3D image of $-\rho_0^n(b_x, b_y)$.

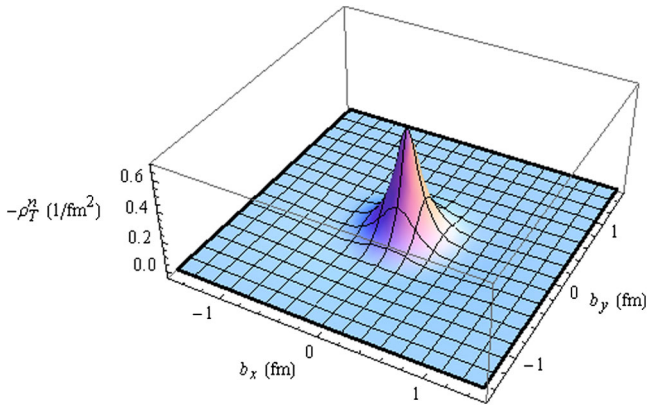

FIG. 20 (color online). 3D image of $-\rho_T^n(b_x, b_y)$.

For completeness in Figs. 11–20 we plot the 2D- and 3D-images of the charge distributions.

V. CONCLUSION

We presented a detailed analysis of the electroproduction of the Roper resonance in the framework of the soft-wall AdS/QCD model. We showed that the Roper mass is mainly generated by the contribution of the leading $3q$ Fock states, and contributions of the higher (4- and 5-partonic) Fock states are small (a similar result was found for the nucleon [17]). In the case of the electroproduction amplitude the leading $3q$ Fock state plays the dominant role and higher Fock states compensate each other. We hope that our predictions will be useful for the JLab experiments and for theoretical investigations on the nature of the Roper resonance.

In the future we plan to apply this formalism to other baryon resonances with adjustable quantum numbers n, J, and L. We suppose that the parameters related to the mixing of the different Fock components are not necessarily the same for all baryons. Therefore, the set of parameters c_τ^B defining the mixing of the Fock components in the specific baryon state and of parameters $c_\tau^{B_1B_2}$ defining the coupling of two Fock components of twist τ in baryons B_1 and B_2 could be varied.

ACKNOWLEDGMENTS

This work was supported by the DFG under Contract No. LY 114/2-1, by the Federal Targeted Program "Scientific and scientific-pedagogical personnel of innovative Russia" Contract No. 02.740.11.0238, by FONDECYT (Chile) under Grant No. 1100287, and by CONICYT (Chile) under Grant No. 7912010025. V. E. L. would like to thank Departamento de Física y Centro Científico Tecnológico de Valparaíso (CCTVal), Universidad Técnica Federico Santa María, Valparaíso, Chile for warm hospitality.

APPENDIX: STRUCTURE INTEGRALS $C_i(Q^2)$

The structure integrals $C_i(Q^2)$ are given by the expressions:

$$C_i(Q^2) = \sum_\tau c_\tau^{\mathcal{R}N} C_i^\tau(Q^2), \tag{A1}$$

$$C_1^\tau(Q^2) = \frac{a}{2} B(a+1, \tau+1)\left(\sqrt{\tau-1}\left(1+\frac{a+1}{\tau}\right)+\sqrt{\tau}\right), \tag{A2}$$

$$C_2^\tau(Q^2) = \frac{a}{2} B(a+1, \tau+1)\left(\sqrt{\tau-1}\left(1+\frac{a+1}{\tau}\right)-\sqrt{\tau}\right), \tag{A3}$$

$$C_3^\tau(Q^2) = \frac{a}{\tau+1} B(a+1, \tau+2)\left(\sqrt{\tau}(1-a\tau) + \sqrt{\tau-1}(a(\tau-1)-1)\left(1+\frac{a+2}{\tau}\right)\right), \tag{A4}$$

$$C_4^\tau(Q^2) = \frac{M_N + M_{\mathcal{R}}}{2} B(a+1, \tau+1)(a(\tau-1) - \tau - 1 + a\sqrt{\tau(\tau-1)}), \tag{A5}$$

where $a = Q^2/(4\kappa^2)$.

[1] I. G. Aznauryan *et al.* (CLAS Collaboration), Phys. Rev. C **80**, 055203 (2009).
[2] V. I. Mokeev *et al.* (CLAS Collaboration), Phys. Rev. C **86**, 035203 (2012).
[3] J. Dudek, R. Ent, R. Essig, K. Kumar, C. Meyer, R. McKeown, Z. E. Meziani, G. A. Miller *et al.*, Eur. Phys. J. A **48**, 187 (2012).
[4] M. B. Gavela, A. Le Yaouanc, L. Oliver, O. Pene, J. C. Raynal, and S. Sood, Phys. Rev. D **21**, 182 (1980); F. E. Close and Z.-P. Li, Phys. Rev. D **42**, 2194 (1990); Z.-P. Li, V. Burkert, and Z.-J. Li, Phys. Rev. D **46**, 70 (1992); D. Robson, Nucl. Phys. **A560**, 389 (1993); F. Cardarelli, E. Pace, G. Salme, and S. Simula, Phys. Lett. B **397**, 13 (1997); U. Meyer, A. J. Buchmann, and A. Faessler, Phys. Lett. B **408**, 19 (1997); Y. B. Dong, K. Shimizu, A. Faessler, and A. J. Buchmann, Phys. Rev. C **60**, 035203 (1999); F. Cano and P. Gonzalez, Phys. Lett. B **431**, 270 (1998); V. D. Burkert and T. S. H. Lee, Int. J. Mod. Phys. E **13**, 1035 (2004); Q. B. Li and D. O. Riska, Phys. Rev. C **74**, 015202 (2006); I. G. Aznauryan, Phys. Rev. C **76**, 025212 (2007); S. Capstick, B. D. Keister, and D. Morel, J. Phys. Conf. Ser. **69**, 012016 (2007); B. Golli, S. Sirca, and M. Fiolhais, Eur. Phys. J. A **42**, 185 (2009); G. Ramalho and K. Tsushima, Phys. Rev. D **81**, 074020 (2010); D. J. Wilson, I. C. Cloet, L. Chang, and C. D. Roberts, Phys. Rev. C **85**, 025205 (2012).
[5] H. J. Weber, Phys. Rev. C **41**, 2783 (1990).
[6] I. G. Aznauryan, Phys. Rev. C **76**, 025212 (2007); I. G. Aznauryan, V. D. Burkert, and T.-S. H. Lee, arXiv:0810.0997.
[7] L. A. Copley, G. Karl, and E. Obryk, Phys. Rev. D **4**, 2844 (1971).
[8] S. Capstick and B. D. Keister, Phys. Rev. D **51**, 3598 (1995).
[9] L. Tiator and M. Vanderhaeghen, Phys. Lett. B **672**, 344 (2009).
[10] I. T. Obukhovsky, A. Faessler, D. K. Fedorov, T. Gutsche, and V. E. Lyubovitskij, Phys. Rev. D **84**, 014004 (2011).
[11] G. F. de Teramond and S. J. Brodsky, AIP Conf. Proc. **1432**, 168 (2012).
[12] I. G. Aznauryan and V. D. Burkert, Prog. Part. Nucl. Phys. **67**, 1 (2012).
[13] I. G. Aznauryan and V. D. Burkert, Phys. Rev. C **85**, 055202 (2012).
[14] I. G. Aznauryan, A. Bashir, V. Braun, S. J. Brodsky, V. D. Burkert, L. Chang, Ch. Chen, B. El-Bennich *et al.*, arXiv:1212.4891.
[15] T. Gutsche, V. E. Lyubovitskij, I. Schmidt, and A. Vega, Phys. Rev. D **85**, 076003 (2012); A. Vega, I. Schmidt, T. Gutsche, and V. E. Lyubovitskij, Phys. Rev. D **83**, 036001 (2011).
[16] T. Branz, T. Gutsche, V. E. Lyubovitskij, I. Schmidt, and A. Vega, Phys. Rev. D **82**, 074022 (2010); A. Vega, I.

Schmidt, T. Branz, T. Gutsche, and V. E. Lyubovitskij, Phys. Rev. D **80**, 055014 (2009); T. Gutsche, V. E. Lyubovitskij, I. Schmidt, and A. Vega, arXiv:1212.5196.

[17] T. Gutsche, V. E. Lyubovitskij, I. Schmidt, and A. Vega, Phys. Rev. D **86**, 036007 (2012).

[18] S. J. Brodsky and G. F. de Teramond, Phys. Rev. Lett. **96**, 201601 (2006).

[19] G. F. de Teramond and S. J. Brodsky, AIP Conf. Proc. **1296**, 128 (2010).

[20] G. F. de Teramond and S. J. Brodsky, Nucl. Phys. B, Proc. Suppl. **199**, 89 (2010).

[21] Z. Abidin and C. E. Carlson, Phys. Rev. D **79**, 115003 (2009).

[22] D. K. Hong, T. Inami, and H. U. Yee, Phys. Lett. B **646**, 165 (2007).

[23] Y. Kim, C. H. Lee, and H. U. Yee, Phys. Rev. D **77**, 085030 (2008); H. C. Ahn, D. K. Hong, C. Park, and S. Siwach, Phys. Rev. D **80**, 054001 (2009); N. Maru and M. Tachibana, Eur. Phys. J. C 63, 123 (2009); H. C. Kim, Y. Kim, and U. Yakhshiev, J. High Energy Phys. 11 (2009) 034; P. Zhang, Phys. Rev. D **81**, 114029 (2010); **82**, 094013 (2010).

[24] A. Kadeer, J. G. Körner, and U. Moosbrugger, Eur. Phys. J. C **59**, 27 (2009).

[25] A. Faessler, T. Gutsche, M. A. Ivanov, J. G. Körner, and V. E. Lyubovitskij, Phys. Rev. D **80**, 034025 (2009).

[26] T. Branz, A. Faessler, T. Gutsche, M. A. Ivanov, J. G. Körner, V. E. Lyubovitskij, and B. Oexl, Phys. Rev. D **81**, 114036 (2010).

[27] H. R. Grigoryan and A. V. Radyushkin, Phys. Rev. D **76**, 095007 (2007).

[28] S. J. Brodsky and G. F. de Teramond, Phys. Rev. D **77**, 056007 (2008).

[29] J. Beringer *et al.* (Particle Data Group), Phys. Rev. D **86**, 010001 (2012).